Kent Academic Repository

Full text document (pdf)

Citation for published version

DOI

Link to record in KAR

https://kar.kent.ac.uk/70048/

Document Version

Author's Accepted Manuscript

Brief communication: disturbances and noise: defining furrow-form enamel hypoplasia

E. Bocaege [1] and S. Hillson[2]

[1] Université de Bordeaux, CNRS, MCC, UMR 5199 PACEA, Équipe A3P, Bâtiment B8, Allée Geoffroy St Hilaire, Pessac Cedex, France

[2] Institute of Archaeology, University College London, London WC1H 0PY, UK

(14 text pages including bibliography, 5 figures)

Abbreviated title: Disturbances and noise

Key words: incremental markings; enamel hypoplasia; three-dimensional analysis; Çatalhöyük

Correspondence to: Emmy Bocaege, Université de Bordeaux, CNRS, MCC, UMR 5199 PACEA, Équipe A3P, Bâtiment B8, Allée Geoffroy St Hilaire, CS 50023, 33615 Pessac Cedex, France. E-mail: e.bocaege@u-bordeaux.fr

Abstract

Objectives

The investigation of the record of growth locked in dental enamel provides a unique opportunity to build a comprehensive picture of growth disruption episodes during childhood. This study presents a new methodological basis for the analysis of enamel growth disruptions (enamel hypoplasia) using incremental microstructures of enamel.

Methods

A three-dimensional technique based upon use of an Alicona 3D Infinite Focus imaging microscope and software is used to record developmental features in the enamel of human permanent mandibular lateral incisors of one individual from the Neolithic site of Çatalhöyük (Turkey). Using this new technique, perikymata are measured down the longitudinal axis of the crown from the incisal margin to the cervix and perikyma spacing profiles are constructed with this new technique. A mathematical basis for the detection of spacing anomalies, which serve as indicators of enamel hypoplasia is presented based upon these profiles.

Results

Three clearly delineated defects were identified visually, then matched and confirmed metrically using the enamel surface and perikyma spacing profiles.

Discussion

Human growth has often been used as an indicator of health in past societies because of developmental sensitivity to fluctuations in nutritional status and disease load. Hence,

standardization of furrow-form defect identification is of crucial importance for reducing the amount of current subjectivity in the determination of a threshold for the identification of defects among individuals of past populations. The method presented here, which is based on microscopic images of the tooth crown as well as recorded measurements of incremental structures, represents a combined visual-metric approach using LOWESS residuals, and as such provides a substantial advancement to previous methods. It is therefore recommended that additional studies be carried out with this methodology to determine whether this method improves the reliability of enamel defect identification among individuals recovered from bioarchaeological contexts.

Enamel hypoplastic defects are deficiencies in enamel thickness that result from physiological perturbations during the formation of tooth crowns (FitzGerald and Saunders, 2005; Goodman and Rose, 1990; Kreshover, 1940; Kronfeld and Schour, 1939; Rose, 1977; Witzel et al., 2008). Enamel grows rhythmically. Among modern humans, there are two rhythms: a circadian (24 hourly) rhythm and rhythm of longer duration that ranges from six to 12 days in different individuals but most commonly lasts between eight and nine days (FitzGerald, 1998; Reid and Dean, 2006; Smith et al., 2010). This latter rhythmic cycle is visible at the crown surface as lines known as perikymata. The spacing of perikymata varies gradually down the longitudinal axis of the crown as part of the normal geometry of crown formation, from around 120 μm apart near the incisal margin, to about 30 μm near the cement-enamel junction (cervix).

Furrow-form defects, the most common type of enamel hypoplasia, result from local variations in this spacing. Usually, a defect is formed by wider than expected spacings between consecutive pairs of perikymata (Guatelli-Steinberg, 2003; Guatelli-Steinberg et al., 2004; Hassett, 2011, 2014; Hillson and Jones, 1989; Hillson, 1992; Hillson and Bond, 1997; King et al., 2002, 2005; Skinner et al., 1995; Temple et al., 2012, 2013; Temple 2014; Witzel et al., 2008). Wider spacings can be observed macroscopically with the naked eye or low−powered microscopy (Buikstra and Ubelaker 1994; Roberts and Connell 2004; Steckel et al., 2006). However, Hassett (2011) argued that the scale of observation introduces an important source of variation in the identification of hypoplastic defects, such that studies based on macroscopic identification are likely to result in the under-recording of defects in the cervical region of the tooth crown.

An alternative method is to define the defects in terms of departures from normal spacing at different points on the crown. A common approach used to determine perikymata spacing is to count the number of perikymata observed within a defined portion of tooth crown height

(for example, perikymata per decile of crown height). One way to do this is by scaling from a scanning electron microscope image of the crown surface under the assumption that the crown surface is perpendicular to the electron beam used to create that image (Hillson, 2014). Another method involves measuring the spacings as seen at the surface in microscopic sections of the crown. It is also possible to use an engineer's measuring microscope to record the positions of perikymata as coordinates along a longitudinal transect down the crown surface (Hassett, 2011, 2014; Hillson and Jones, 1989; King et al., 2002, 2005).

More recently, optical profilometry has been used to create three-dimensional models of the crown surface, from which perikymata can be counted and their spacing measured (Bocaege et al., 2010; Elhechmi, 2010; Elhechmi et al., 2013; Le Cabec et al., 2015). These counts and measurements can then be used to calculate the average perikyma spacing within that specific region of the crown surface (Dean and Reid, 2001; Guatelli-Steinberg et al., 2005, 2007, 2012; Ramirez Rozzi and Bermudez de Castro, 2004; Reid and Dean, 2000). Using coordinates to calculate direct spacings, rather than perikyma counts, has the added advantage of allowing a comparison between the actual perikyma spacing and the underlying longitudinal trend in perikyma spacing along the crown surface (Bocaege et al., 2010; Hillson and Jones, 1989; Hassett, 2011, 2014; Hillson 1992a; King et al., 2002, 2005; Temple et al., 2012, 2013).

However, the detection of anomalies in the overall perikyma spacing trend is not straightforward, for the definition of furrow-form defects based upon perikyma spacing varies considerably. Some studies focus on a visual identification, with the lower limits of defects identified as grooves that appear larger than adjacent perikyma grooves under low-power (10x) magnification (Guatelli-Steinberg 2003; Hillson 1992b; King et al., 2002, 2005; Temple 2010; Witzel et al., 2008). Another approach is to establish a perikyma spacing average above which large spacings are considered to be defects. For example, Temple (2012) defines "accentuated perikymata" as those greater than 100µm apart in the occlusal part of the tooth, wider than 70µm in the midregion of the crown and 50µm in the cervical region. A more specific threshold has been put forward by Hassett (2011), who used Z-scores to identify these "accentuated perikymata".

The main difficulty in setting such a threshold relates to the variation in perikyma spacing between different parts of the crown. First, there is a general decrease in spacing as one proceeds from the incisal margin to the cervical region of the crown. This trend is largely a consequence of a change in the angular relationships between the regular layering and other

3

elements of enamel structure, due to the fact that the tooth crown grows in height (so-called enamel extension rate) more rapidly near the cusps than it does near the cervix (Dean and Reid, 2001, Guatelli-Steinberg et al., 2012). As a result, perikymata spacings are always widest near the incisal margin and decrease gradually down to the longitudinal axis of the crown to the cervix.

Another issue is the variation in spacing around the circumference of the crown. For example, a recent study compared the spacing between equivalent pairs of perikymata across the transverse axis of the crown of a lower central incisor and found that the perikyma spacing varied in a particularly striking way between various locations along this axis, ranging from a spacing of 5 μm in the center of the crown's transverse axis to a spacing of 40 μm at the mesial and distal margins of this axis (Bocaege et al., 2010). These trends are a normal part of tooth crown anatomy and, in order to identify developmental defects, their effects needs to be filtered out from the general trend.

If an analogy is made with signal processing, developmental defects of enamel can be likened to noise and the normal spacing trend of the main signal. Noise can be identified as short-term fluctuations superimposed upon smoother long-term fluctuations in the signal (O'Haver, 2013). Noise is reduced in signal processing by the use of a variety of mathematical smoothing procedures applied to the signal data. As well as reducing noise in, for example, a radio signal, it is also possible to apply this approach to complex time series such as rainfall records. A moving average may be used to highlight long-term trends amongst the clutter of variation in daily rainfall measurements (Longobardi and Villani, 2010). This might for example be calculated for each day as the mean of the week's readings either side of it. Hassett (2011) used a similar approach to isolate the normal trend of perikymata spacing down the longitudinal axis of the crown, in which at each perikyma groove, the mean and standard deviation of spacings in its nearest 10 neighbors was calculated. This moving average summarized the normal spacing trend down the longitudinal axis of the crown side and defects were defined as perikymata spacings that departed by more than two standard deviations from the value of the running mean.

The difficulty with a simple running mean of this kind is that even slight irregularities in the crown mean that neighboring spacing profiles of the same perikymata can produce quite different results. Here we propose to minimize this additional source of noise by expressing perikyma spacing in terms of distance from the first identified perikyma groove (Hillson, 2014). That is, the distance to each successive perikyma groove is added to the sum of all

previous distances. In this way, distances between perikyma grooves are not assessed individually, but considered as part of the cumulative process resulting in the final height of the crown. This cumulative spacing is a better guide to the progression of crown development right around its circumference. A longitudinal growth curve is constructed when these cumulative perikymata measurements are plotted against time (in terms of perikymata counts). One can then define curves that provide the best fit to the dispersion of cumulative perikymata measurements against time in order to capture the underlying 'normal' trend of tooth growth. As such, departures from the normal trend are expressed as residuals, and this is the approach used in this paper.

MATERIALS AND METHOD

Enamel defects were observed in the anterior dentition of a seven year-old child recovered from the Neolithic site of Çatalhöyük, located on the Konya plain of Turkey and dates between 7400-7100 BC to 6200-5900 BC (Hodder, 2013). The individual (CH 6682) was buried under the floor of Building 3 (Bach area), in the west part of the main room. The skeleton was found complete and in articulation with no identifiable skeletal pathology (Molleson et al., 2005).

The tooth crowns were cleaned using acetone-impregnated cotton swabs. Coltène President's Jet Light Body Plus (polyvinylsiloxane), was applied to the entire crown surface with a spatula. After curing, impressions were gently released from the teeth and kept in plastic bags to protect them from dust. Positive casts of the entire crown surface were made using Epotek 301 epoxy resin and covered with a gold sputter-coating.

The tooth replicas were studied with the Alicona Infinite Focus, a three-dimensional measuring microscope (Bocaege et al., 2010). A compromise between long scanning times and image resolution was achieved by scanning coated replicas of the tooth crowns with a 5x objective lens, which produced images in which perikymata could be clearly identified and measured. Images of the tooth crowns were captured along the longitudinal axis of the crown from the incisal margin to the cement-enamel junction, along the mid-sagittal surface using a vertical resolution of 8μm and a lateral resolution of 1.75 x 1.75 μm. This allowed the capture of the entire tooth crown in one scan thereby avoiding any bias introduced by overlapping fields of view.

Clearly delineated defects where initially identified visually on the microscopic images. After this, a profile line was drawn down the image and this appeared as a graph underneath, with the transverse axis recording the distance along the profile and the longitudinal axis the

relative height of the surface. The vertical relief of the perikymata proved very small, measuring only fractions of a micrometer, so they were not always recognizable in the profile. Instead, the image was used to identify the positions of the perikyma grooves along the profile line. A cursor matched these positions on the profile graph and it was possible to determine the transverse and longitudinal coordinates of each one. With a profile line drawn down the vertical axis of the tooth crown, this process was repeated from the first visible perikyma near the central mamelon to the cemento-enamel junction at the cervical base of the crown. The rendered image of the crown surface model was exported as a JPEG file and each recorded perikyma groove was labelled on this exported image, so that it could be compared directly with graphs of the measured spacings.

The spacing between pairs of perikyma grooves was calculated by simple application of the Pythagorean formula to the transverse and longitudinal coordinates. In addition, cumulative spacing was calculated by continuously adding the pair-by-pair spacing, from the incisal to cervical margins (perikyma 1 to 156). The overall amount of cumulative growth was determined by fitting a locally weighted scatter plot smoothed (LOWESS) curve to the data points.

LOWESS has a previous history of success in modelling primate growth and hominoid canine extension rates (Leigh, 1992, 1996; Schwartz and Dean, 2001). It is a non-parametric method that fits parametric functions to localized subsets of the independent variables using weighted least squares in a moving fashion, similar to the way a time series is smoothed by moving averages (Cleveland and Devlin, 1988; Cleveland and Grosse, 1991; Jacoby, 2000; Kohler et al., 2008).

Linearity is assumed over short, local sets of data when using non-parametric approaches such as LOWESS fitting (Moses et al., 1992). In essence, LOWESS is a method for fitting a regression relationship to noisy data (Cleveland and Grosse, 1991; Downey et al., 2014; Jacoby, 2000; Kohler et al., 2008) and is therefore a good match for the cumulative perikymata spacing curves produced in this study.   Additionally, as the LOWESS method requires fairly large and sampled datasets in order to produce robust models, cumulative perikyma spacing curves make a good application (Guthrie, 2012).

Alpha parameters control the group of neighboring points included in the LOWESS regression at each perikyma groove. Various alpha values were tested to minimize the chance of over-fitting. An investigation of the scatter plots confirms that the use of alpha parameter 0.1 is reasonable, as smoothing parameters above 0.1 fail to compensate for the

underlying trend of wider perikymata in the incisal part of the crown relative to the cervical region of the crown (Fig. 1). The resulting LOWESS curve with alpha set at 0.1 allows the observer to take individual perikymata spacing measurements in different regions of the crown and render them comparable (Moses et al., 1992).

Residuals were calculated for each perikyma groove as the difference of the observed value to the predicted value given by the LOWESS curve for that point. Spacings that are large relative to neighboring perikymata spacings yield positive residuals, while those spacings that are relatively small produce negative residuals (Moses et al., 1992).
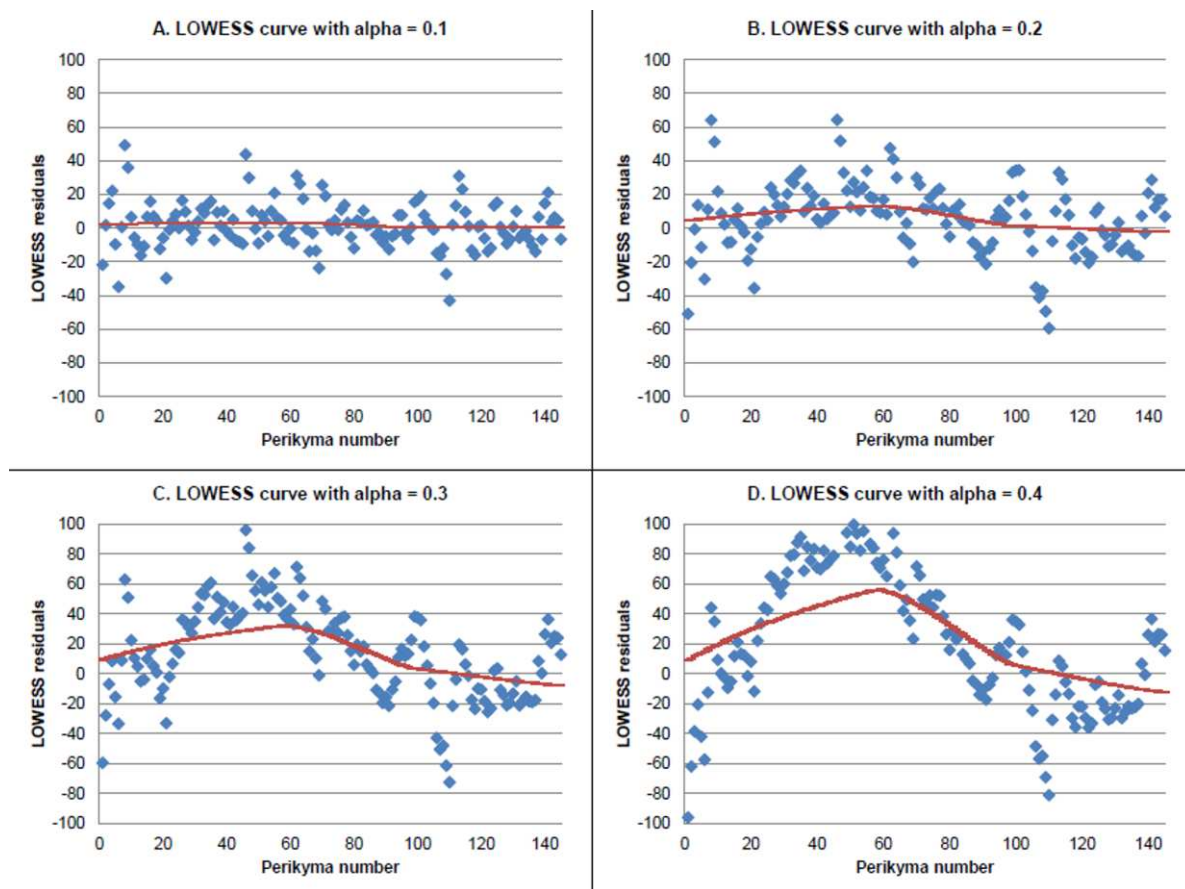

Figure 1: Effect of the alpha parameter on the LOWESS residuals. Residual plots from LOWESS curve fitted to cumulative perikyma spacings using alpha values of 0.1, 0.2, 0.3 and 0.4 corresponding to 15, 30, 45, 60 neighboring points. Solid red line is LOWESS curve fitted to the residuals using an alpha value of 0.75 (method based on Jacoby 2000)

If developmental defects are defined as perikyma spacings that are larger than normal at a given point along the longitudinal axis of the crown, such defects ought to stand apart with unusually high residual values (Moses et al., 1992). It was therefore necessary to find a threshold above which values could be classed as abnormally high. This was accomplished based upon percentiles for the combined residual values, such that values at or above the

90th percentile, commonly defined as threshold criteria in the medical literature (Hediger et al., 1998; Messiah et al., 2010), were considered abnormally high.

RESULTS

An intra-observer error study for perikyma counts was carried out based on the method outlined by Guatelli-Steinberg (2003) to compare observer reliability in the current study with those obtained in previous studies. Briefly, a profile line equivalent to 1mm was drawn along the longitudinal axis of the lower lateral incisor from the incisal margin of the crown to the cervical base of the crown. Perikymata along this line for 20 teeth from the Çatalhöyük dental assemblage (two teeth per randomly chosen individual) were scored on two separate occasions (two weeks apart). Similarly to Guatelli-Steinberg (2003), percent error was calculated in accordance with the method of Calcagno (1989), in which the difference in measurement pairs is expressed as a proportion of the first measurement. The total of these values are then divided by the number of teeth considered (20) and multiplied by 100 to give the percent error.

In this error study, the sum of values amounts to 0.39, corresponding to a percent error of 1.96%. As such, the results from this quantitative analysis indicate an intra-observer error of less than 2% for perikymata counts, which is lower than the previously reported error rates of 5% and 2.4% by Dean et al. (2001) and Guatelli-Steinberg (2003) respectively.

Microscopic images of two antimeric lower lateral incisors were visually assessed for clear and well-delineated defects and the visually identified defects (Fig. 2) were confirmed by assessing enamel surface profiles and perikyma spacing profiles (Fig. 3). More specifically, three clearly delineated defects were detected that could be matched between the antimeres. defect A corresponds to perikymata 45 to 51, defect B to perikymata 68 to 75 and defect C to perikymata 96-103.
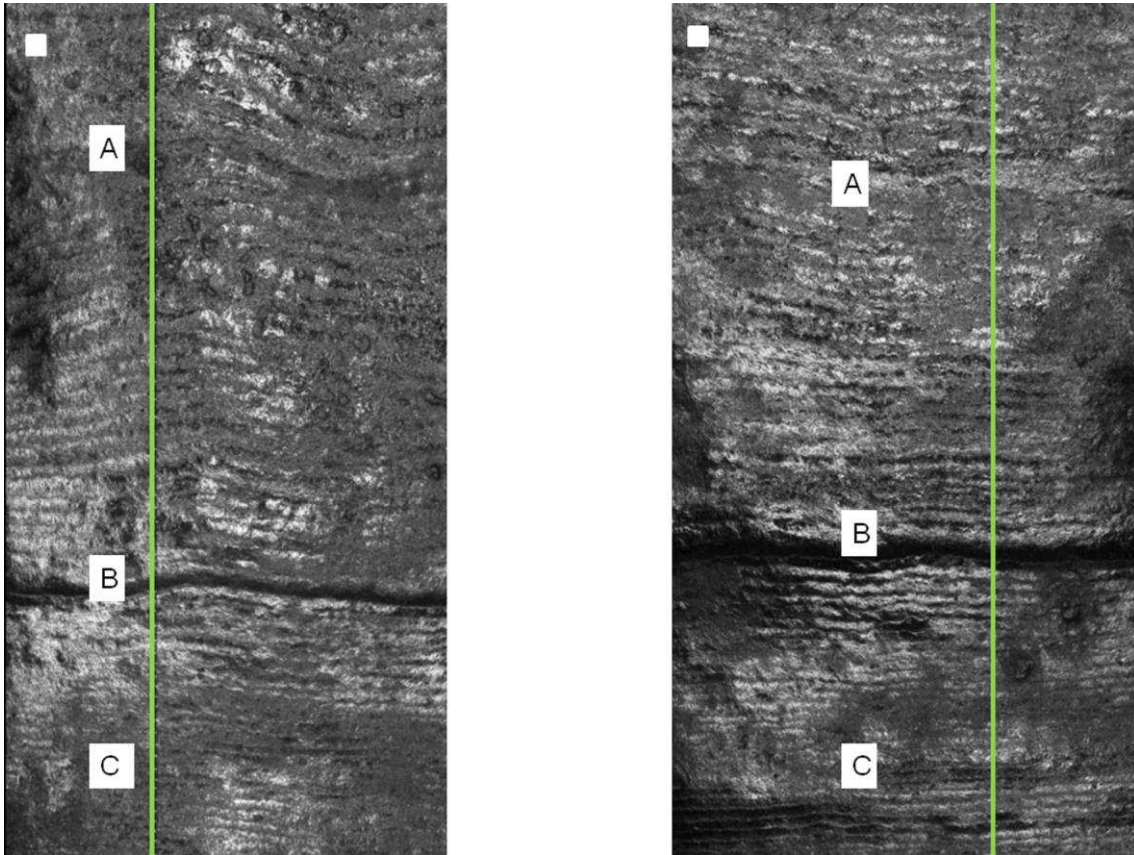
Figure 2: Image of the mid-to occlusal parts of the lower right and left lateral incisors (CH 6682). Letters correspond to visually identified matching defects. Solid green line is profile line drawn down the longitudinal axis of the tooth crown, from the first visible perikyma groove near the incisal margin to the last groove at the cervical base of the crown. Scale = 200µm

Figure 3 represents the enamel surface and perikyma spacing profile for the lower left lateral incisor. The count of perikymata is shown along the horizontal axis, the raw individual perikyma spacings (in black) and the enamel surface based on the longitudinal coordinates are shown along the y-axis (in gray). The graphs representing the longitudinal coordinates typically appear slightly bulging, following the labial bulge of the incisor crown in profile. Furrow-form defects of enamel hypoplasia are characterized by depressions in the enamel surface, and as such, visually identified enamel defects A and C can be clearly identified as indentations within such surface graphs which can be linked to increased individual perikyma spacings (Fig. 3). The indentation in the crown surface corresponding to visually identified defect B is less obvious, but nevertheless represents a more dramatic decrease in depth relative to neighboring regions that do not correspond to increased perikymata spacing.
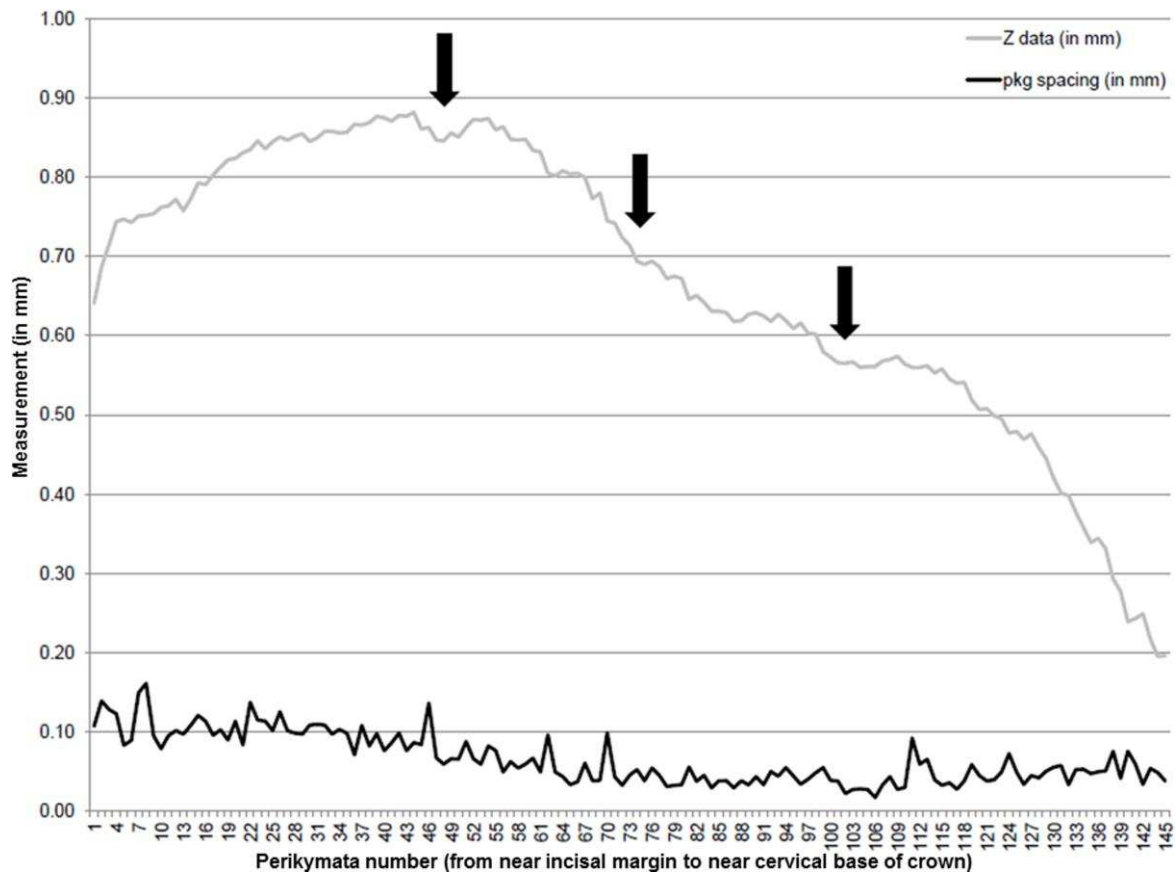
Figure 3: Enamel surface (grey) and perikyma spacing (black) profile for lower left lateral incisor (CH 6682). Black arrows indicate visually identified defects

In Figure 4, the residual values calculated from the fitted LOWESS curve for the lower left lateral incisor are represented using a box and whiskers plot. Here we adopt the 10th and 90th percentile for the ends of the whiskers (as per Banacos, 2011). Residual values vary from a maximum of 64 to a minimum of around -60, with the median at 8 and the 90th percentile at 31. Residual values for the perikymata within defects A, B, C stand out clearly as outliers above the upper whisker. In contrast to the enamel surface profile or the perikymata spacing profile, where the location of defects is not always obvious, the residual approach identifies these three defects clearly and objectively. As to the negative outliers, two of these (-40.21 and -50.95) represent the endpoints of the smoothed curve: as such, they may be considered noise. The two other outliers likely represent the range of normal variation present in perikyma spacing; similar extremely small spacings have been identified previously (Bocaege et al., 2010).

75.00 — 64.26 (Defect A)

55.00 — 47.44 (Defect B)

35.00 — 34.42 (Defect C)

LOWESS residuals — 8.11

-30.31727412
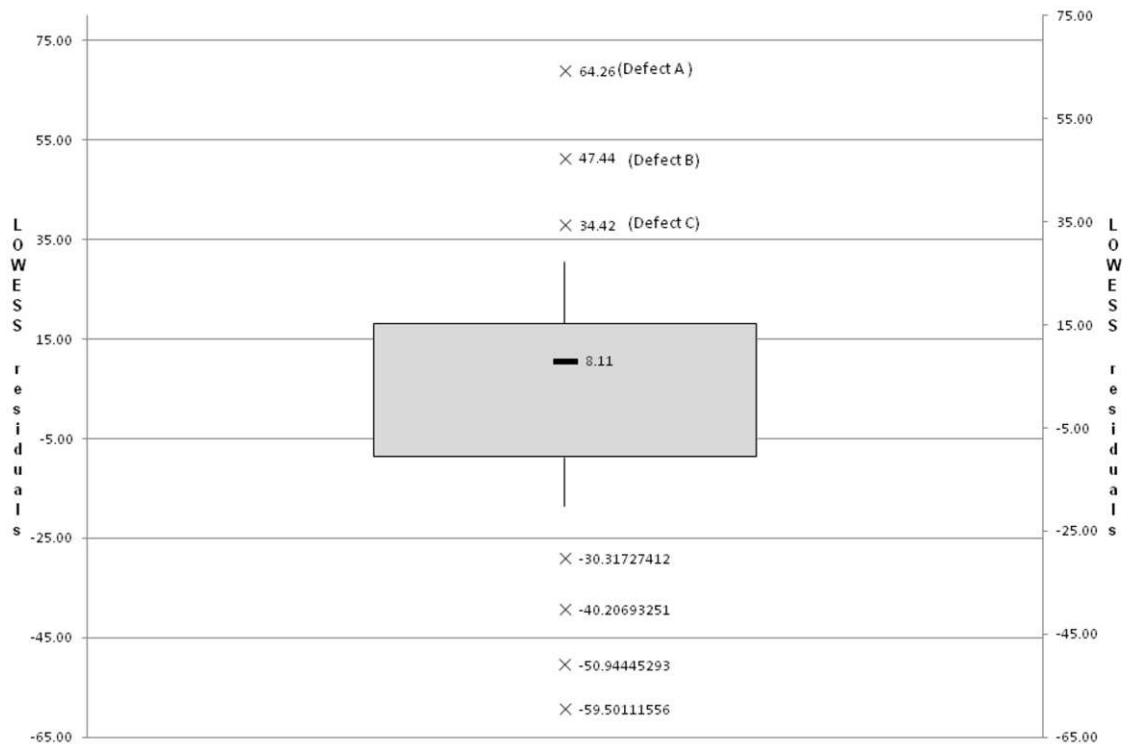
-40.20693251

-50.94445293

-59.50111556

Figure 4: Box and whiskers plot depicting the residual values calculated from the fitted LOWESS curve for the lower left lateral incisor. The height of the box extends from the 25th to 75th percentile. The horizontal bar within the box is the median value. The end of the whiskers represents 10th and 90th percentiles, respectively. Defects A, B and C are labeled with an "x".

Identified defects A, B and C were matched with teeth with overlapping developmental schedules (Hassett 2011; Hillson and Bond 1997; King et al. 2002, 2005; Reid and Dean 2000) to confirm that these defects were caused by a systemic disturbance rather than localised trauma. Similar spacing anomalies (which equally stood out as outliers above the set threshold) were detected in corresponding regions in the permanent lower central incisor, upper central incisor and upper lateral incisor (Fig. 5). However, while all incisor types yield evidence of a defect that corresponds in timing with Defect A, only the maxillary teeth yield evidence for a defect that corresponds to Defect B and only the mandibular teeth provide corroboratory evidence for Defect C.

Figure 5: Perikyma groove counts and defect matches for the permanent lower lateral incisors, lower central incisor, upper central incisor and upper lateral incisor. Black full circles represent first, last and every tenth perikymata, blue full circles represent matched defects.

DISCUSSION

Perikyma spacing profiles were constructed for antimeres of one individual in order to determine whether a mathematical approach, in addition to a visual inspection of microscopic images and enamel surface profiles, can be used to reconstruct growth patterns in human dental remains and to remove some of the subjectivity associated with the visual identification of defect presence across dentitions.

Three clearly delineated defects on the antimeric mandibular lateral incisors of individual CH6682 were identified visually and confirmed metrically using the enamel surface and perikymata spacing profiles. However, only one of these defects (Defect A) could be matched between upper and lower incisors, whereas defect B and C could only be matched with the maxillary incisors and lower central incisor respectively. The matching of defects between some teeth but not others has been referred to in the anthropological literature (King et al. 2002, 2005; Temple 2012), but the reason behind this lack of matching has not yet been studied in detail. As such, there is a need for more studies regarding this issue in order to establish whether this lack of defect matching is physiological or methodological.

In terms of imaging, the threedimensional technique (Alicona 3D Infinite Focus imaging microscope and software) constitutes a substantial advance to the engineer's microscope method (Hassett, 2011; Hillson and Jones, 1989; King et al., 2002, 2005; Temple et al., 2012, 2013). This is because, in contrast to the engineer's measuring microscope, the Infinite Focus imaging microscope allows on-screen visualization of perikymata morphology, which enhances the subsequent identification of perikymata grooves. Still further, and again in contrast to the engineer's microscope (used in conjunction with SEM images), the Infinite Focus imaging microscope not only allows direct on-screen comparisons to be made between measurements and images, but also allows for the export of high resolution images as a permanent record for future use (with different software if required).

Nevertheless, a current limitation of the method is the cost of the Alicona instrument and software. Possibilities for future research include comparisons between the assessment of three−dimensional models using available analytical freeware and the Alicona proprietary software as well as comparisons with other three-dimensional imaging techniques such as SEM (Alicona MeX) and Polynomial Texture Mapping (PTM) domes.

The standardization of furrow-form defect identification is of crucial importance for reducing the current substantial bias in the bioarchaeological assessment of health in the past. This preliminary study sets for a method for obtaining objective, microscopic identifications of such defects in human dentitions by creating permanent records and working towards the standardization of recording methods.

Based on the results of this case study, a combined visual - metric approach using LOWESS residuals is recommended for the identification of enamel defects. This technique, which is based on images of the tooth crown as well as recorded measurements, has the potential to reduce the level of subjectivity in the analysis of crown surface characteristics. On the basis of this method, identified defects can then be matched across the dentition and interpreted based upon comparisons between dentitions from individuals buried in different bioarchaeological and palaeoanthropological contexts. A larger study comparing different metric methods (such as LOWESS and running means) and using a larger sample will determine which method is best suited to reliably detect enamel defects.

This study was limited to recording enamel defects on incisors, but the method could be easily adapted to detect anomalies in the perikyma spacing of other tooth types. Continuing

work on other individuals in the Çatalhöyük dental assemblage and other dental assemblages can determine whether this threshold is confirmed, as well as assessing the limits to which perikymata can be observed on worn teeth.

ACKNOWLEDGEMENTS

LITERATURE CITED

Banacos PC. 2011. Box and whisker plots for local climate datasets: Interpretation and creation using Excel 2007/2010. NWS Eastern Region Technical Attachment No. 2011-01. New York: National Weather Service, Eastern Region Headquarters.

Bocaege E, Humphrey LT and Hillson SW. 2010. Technical note: a new three−dimensional technique for high resolution quantitative recording of perikymata. Am J Phys Anthropol 141: 498−503.

Buikstra JE, Ubelaker DH. 1994. Standards for data collection from human skeletal remains. Arkansas, Fayetteville, AR: Archaeological Survey Research Series No 44

Calcagno JM. 1989. Mechanisms of dental reduction: a case study from post−Pleistocene Nubia. Lawrence: University of Kansas Publications in Anthropology Volume 18

Cleveland WS, Devlin SJ. 1988. Locally weighted regression: an approach to regression analysis by local fitting. J Am Stat Assoc 83(403): 596−610.

Cleveland WS, Grosse E. 1991. Computational methods for local regression. Stat Comp 1: 47−62.

Dean MC, Leakey MG, Reid D, Schrenk F, Schwartz G, Stringer C, Walker A. 2001. Growth processes in teeth distinguish modern humans from Homo erectus and earlier hominins. Nature 414: 628−631.

Dean MC, Reid DJ. 2001. Perikymata spacing and distribution on hominid anterior teeth. Am J Phys Anthropol 116: 209−215.

Downey SS, Bocaege E, Kerig T, Edinborough K, Shennan S. 2014. The neolithic demographic transition in Europe: correlation with juvenility index supports interpretation of the Summed Calibrated Radiocarbon Date Probability Distribution (SCDPD) as a valid demographic proxy. PloS one, 9(8): e105730.

Elhechmi I. 2010. Instrumentation optique pour la mesure des périkymaties de la couronne dentaire. Unpublished Ph.D. thesis, Universite de Franche−Comte.

Elhechmi I, Braga J, Dasgupta G, Gharbi T, 2013. Accelerated measurement of perikymata by an optical instrument. Biomed Opt Express 4(10): 2124−2137.

FitzGerald CM. 1998. Do enamel microstructures have regular time dependency? Conclusions from the literature and a large−scale study. J Hum Evol 35: 371–386.

FitzGerald CM, Saunders SR. 2005. Test of histological methods of determining chronology of accentuated striae in deciduous teeth. Am J Phys Anthropol 127: 277–290.

Goodman AH, Rose JC. 1990. Assessment of systemic physiological disturbances from dental enamel hypoplasia and associated histological structures. Yearb Phys Anthropol 33: 59−110.

Guatelli−Steinberg D. 2003. Macroscopic and microscopic analyses of linear enamel hypoplasia in Plio Pleistocene South African Hominins with respect to aspects of enamel development and morphology. Am J Phys Anthropol 120: 309−322.

Guatelli-Steinberg D, Larsen CS, Hutchinson DL. 2004. Prevalence and the duration of linear enamel hypoplasia: a comparative study of Neandertals and Inuit foragers. J Hum Evol 47(1): 65-84.

Guatelli−Steinberg D, Reid DJ, Bishop TA, Larsen CS. 2005. Anterior tooth growth periods in Neanderthals were comparable to those of modern humans. PNAS 102(40): 14197−14202.

Guatelli−Steinberg D, Reid DJ, Bishop TA. 2007. Did the lateral enamel of Neanderthal anterior teeth grow differently from that of modern humans? J Hum Evol 52: 72−84.

Guatelli-Steinberg D, Floyd BA, Dean MC, Reid DJ. 2012. Enamel extension rate patterns in modern human teeth: two approaches designed to establish an integrated comparative context for fossil primates. J Hum Evol 63(3): 475-486.

Guthrie W. 2012. Process modeling. In NIST Engineering Statistics Handbook. http://www.itl.nist.gov/div898/handbook/pmd/section1/pmd144.htm (retrieved on 27/05/13)

Hassett BR. 2011. Evaluating sources of variation in the identification of linear hypoplastic defects of enamel: a new quantified method. J Archaeol Sci 39: 560−565.

Hassett BR. 2014. Missing defects? A comparison of microscopic and macroscopic approaches to identifying linear enamel hypoplasia. Am J of Phys Anthropol 153(3): 463-472.

Hediger ML, Overpeck MD, Maurer KR, Kuczmarski RJ, McGlynn A, Davis WW. 1998. Growth of infants and young children born small or large for gestational age: findings from the Third National Health and Nutrition Examination Survey. Arch Pediatr Adolesc Med 152(12): 1225-1231.

Hillson SW, Jones BK. 1989. Instruments for measuring surface profiles: an application in the study of ancient human tooth crown surfaces. J Archaeol Sci 16: 95−105.

Hillson SW. 1992a. Impression and replica methods for studying hypoplasia and perikymata on human tooth crown surfaces from archaeological sites. Int J Osteoarchaeol 2: 65−78.

Hillson SW. 1992b. Dental enamel growth, perikymata and hypoplasia in ancient tooth crowns. J R Soc Med 85: 460-466.

Hillson SW, Bond S. 1997. Relationship of enamel hypoplasia to the pattern of tooth crown growth: a discussion. Am J Phys Anthropol 104: 89−103.

Hillson SW. 2014. Tooth development in human evolution and bioarchaeology. Cambridge: Cambridge University Press

Hodder I., Çatalhöyük research project. 2013. Humans and landscapes of Çatalhöyük: reports from the 2000-2008 seasons. British Institute at Ankara; Cotsen Institute of Archaeology at UCLA.

Jacoby WG. 2000. Loess: a nonparametric, graphical tool for depicting relationships between variables. Elect Stud 19: 577−613.

King T, Hillson SW, Humphrey L. 2002. A detailed study of enamel hypoplasia in a post−medieval adolescent of known age and sex. Arch Oral Biol 47: 29−39

King T, Humphrey L, Hillson SW. 2005. Linear enamel hypoplasias as indicators of systemic physiological stress: evidence from two known age−at−death and sex populations from Postmedieval London. Am J Phys Anthropol 128: 547−559.

Kohler TA, Glaud MP, Bocquet−Appel JP, Kemp BM. 2008. The Neolithic demographic transition in the US Southwest. Am Antiq 73(4): 645−669.

Kreshover SJ. 1940. Histopathologic studies of abnormal enamel formation in human teeth. Am J Orthod Oral Surg 26: 1083−1101.

Kronfeld R, Schour I. 1939. Neonatal dental hypoplasia. J Am Dent Assoc 26: 18−32.

Le Cabec A, Tang N, Tafforeau P. 2015. Accessing developmental information of fossil hominin teeth using new synchrotron microtomography-based visualization techniques of dental surfaces and interfaces. PloS one 10(4): e0123019.

Leigh SR. 1992. Patterns of variation in the ontogeny of primate body size dimorphism. J Hum Evol 23: 27−50.

Leigh SR. 1996. Evolution of human growth spurts. Am J Phys Anthropol 101(4): 455−474.

Longobardi A, Villani P. 2010. Trend analysis of annual and seasonal rainfall time series in the Mediterranean area. Int J Climatol 30(10): 1538−1546.

Messiah SE, Arheart KL, Lipshultz SE, Miller TL. 2010. Prevalence of the metabolic syndrome in US Youth. In: Bagchi D, editor. Global perspectives on childhood obesity: current status, consequences and prevention. London: Academic Press, p. 107−119.

Molleson T, Andrews P, Boz B. 2005. Reconstruction of the Neolithic people at Catalhoyuk. In: Hodder I, editor. Inhabiting Çatalhöyük: reports from the 1995−1999 seasons. (McDonald Institute Monographs). Cambridge: McDonald Institute for Archaeological Research; London: British Institute of Archaeology at Ankara, p. 279−301.

Moses LE, Gale LC, Altmann J. 1992. Methods for analysis of unbalanced, longitudinal growth data. Am J Primatol 28: 49–59.

O'Haver T. 2013. A pragmatic introduction to signal processing with applications in chemical analysis. http://terpconnect.umd.edu/~toh/spectrum/TOC.html (retrieved on 24/05/14).

Ramirez–Rozzi F, Bermudez de Castro J. 2004. Surprisingly rapid growth in Neanderthals. Nature 428: 935–939.

Reid DJ, Dean MC. 2000. Brief communication: the timing of linear enamel hypoplasias on human anterior teeth. Am J Phys Anthropol 113: 135–139.

Reid DJ, Dean MC. 2006. Variation in modern human enamel formation times. J Hum Evol 50: 329–346.

Roberts, C.A. and Connell, B., 2004. Guidance on recording palaeopathology. In: Guidelines to the standards for recording human remains. Southampton/Reading: British association for biological anthropology and osteoarchaeology and Institute of field archaeology, p. 34–39

Rose JC. 1977. Defective enamel histology of prehistoric teeth from Illinois. Am J Phys Anthropol 46: 439–446.

Schwartz GT, Dean CM. 2001.Ontogeny of canine dimorphism in extant hominoids. Am J Phys Anthropol 115: 269–283.

Skinner MF, Dupras TL, Moya–Sola S. 1995. Periodicity of enamel hypoplasia among Miocene Dryopithecus from Spain. J Paleopathol 7: 197–222.

Smith TM, Tafforeau P, Reid DJ, Pouech J, Lazzai V, Zermeno JP, Guatelli–Steinberg D, Olejniczak AJ, Hoffman A, Radov J, Makaremi M, Toussaint M, Stringer C, Hublin J–J. 2010. Dental evidence for ontogenetic differences between modern humans and Neanderthals. PNAS 107(49): 20923–20928.

Steckel RH, Larsen CS, Sciulli PW, Walker PL. 2006. Data collection codebook. In: R.H. Steckel RH, Larsen CS, Sciulli PW, Walker PL, editors. The global history of health project. http://global.sbs.ohio–state.edu/new_docs/Codebook_08_25_05.pdf (retrieved on 10/05/14)

Temple DH. 2010. Patterns of systemic stress during the agricultural transition in prehistoric Japan. Am J Phys Anthropol 142: 112–124

Temple DH, Nakatsukasa M, Mcgroarty JN. 2012 Reconstructing patterns of systemic stress in a Jomon period subadult using incremental microstructures of enamel. J Archaeol Sci 39(5): 1634–1641.

Temple DH, McGroarty JN, Guatelli–Steinberg D, Nakatsukasa M, Matsumura H. 2013. A comparative study of stress episode prevalence and duration among Jomon period foragers from Hokkaido. Am J Phys Anthropol 152(2): 230–238.

Temple DH. 2014. Plasticity and constraint in response to early-life stressors among late/final jomon period foragers from Japan: Evidence for life history trade-offs from incremental microstructures of enamel. Am J Phys Anthropol 155(4): 537-545.

Witzel C, Kierdorf U, Schultz M, Kierdorf H. 2008. Insights from the inside: histological analysis of abnormal enamel microstructure associated with hypoplastic enamel defects in human teeth. Am J Phys Anthropol 136(4): 400−414.